BMC Genomics

RESEARCH

Open Access

A dual sgRNA library design to probe genetic modifiers using genome-wide CRISPRi screens

Alina Guna[1,2†], Katharine R. Page[1†], Joseph M. Replogle[2,3,4], Theodore K. Esantsi[2,4], Maxine L. Wang[1,2], Jonathan S. Weissman[2,4,5,6] and Rebecca M. Voorhees[1,7*]

Abstract

Mapping genetic interactions is essential for determining gene function and defining novel biological pathways. We report a simple to use CRISPR interference (CRISPRi) based platform, compatible with Fluorescence Activated Cell Sorting (FACS)-based reporter screens, to query epistatic relationships at scale. This is enabled by a flexible dual-sgRNA library design that allows for the simultaneous delivery and selection of a fixed sgRNA and a second randomized guide, comprised of a genome-wide library, with a single transduction. We use this approach to identify epistatic relationships for a defined biological pathway, showing both increased sensitivity and specificity than traditional growth screening approaches.

Keywords CRISPR interference, Genetic modifier, Epistasis, Genome-wide screen, ER membrane protein complex, Tail-anchored proteins

Introduction

In higher eukaryotes, complex phenotypes are facilitated not only by genetic expansion, but by the combinatorial effects of genes working in concert [1, 2]. Evolutionarily, this complexity affords both genetic redundancy and the ability to undergo rapid cellular adaptation, which ensures phenotypic robustness upon loss or mutation of any particular gene. Indeed, most fundamental processes are buffered by components with partially overlapping function including protein quality control (i.e. protein folding chaperones and E3 ubiquitin ligases), cellular stress response (i.e. the heat shock response and the ubiquitin-proteasome system), and protein biogenesis (i.e. targeting and insertion to the endoplasmic reticulum [ER]) [3–7]. However, this creates technical challenges to genetically interrogating biological pathways and assigning gene function in mammalian cells. For example, only ~ 1/4 of the ~ 10,000 genes expressed in a typical cell will result in any detectable growth phenotype when depleted [8–11].

†Alina Guna and Katharine R. Page contributed equally to this work.

*Correspondence:
Rebecca M. Voorhees
voorhees@caltech.edu
[1]Division of Biology and Biological Engineering, California Institute of Technology, 1200 E. California Ave, Pasadena, CA 91125, USA
[2]Whitehead Institute for Biomedical Research, Massachusetts Institute of Technology, Cambridge, MA 02142, USA
[3]Medical Scientist Training Program, University of California, San Francisco, San Francisco, CA 94158, USA
[4]Howard Hughes Medical Institute, Massachusetts Institute of Technology, Cambridge, MA 02142, USA
[5]Department of Biology, Massachusetts Institute of Technology, Cambridge, MA 02142, USA
[6]David H. Koch Institute for Integrative Cancer Research, Massachusetts Institute of Technology, Cambridge, MA 02142, USA
[7]Howard Hughes Medical Institute Freeman Hrabowski Scholar, California Institute of Technology, Pasadena, CA 91125, USA

To address these challenges, genetic modifier screens have traditionally been a powerful tool for defining gene function, identifying missing components of known pathways, establishing disease mechanisms, and pinpointing new drug targets [12–20]. Forward genetic modifier screens rely on genetic 'anchor points' as a baseline for determining whether subsequent mutations, generally induced through random mutagenesis, result in buffering or synthetic phenotypes. In practice, this 'anchor' is established in a model organism or cell, often requiring extensive manipulation to generate a specific knockout in either organisms or cells, or isogenic mutant cell lines [21–23]. Apart from being technically cumbersome, classic forward approaches lack the ability to systematically assess genetic interactions on a genome-wide scale. The advent of CRISPR-based techniques has expanded this ability by allowing for (i) the generation of specific genetic perturbations in the form of knockouts or knockdowns and (ii) the performance of unbiased genome-wide forward genetic screens to identify the genetic basis of an observed phenotype.

The majority of genetic modifier screens in human cells leverage a CRISPR cutting based approach [24–28]. However, Cas9-mediated DNA cutting is toxic to cells because it activates the DNA damage response, which is fundamentally problematic for genetic interaction analysis where multiple genomic sites are targeted [29, 30]. Additionally, cells readily adapt and compensate for loss-of-function mutations over time, diminishing observed phenotypes when isogenic knockout cell lines are required [31]. Moreover, relying on a genetic knockout approach is often not amenable to the study of essential genes. A more acute strategy, CRISPR interference (CRISPRi), circumvents many of these issues and offers several advantages, notably the ability to create homogenous, titratable knockdown of genes without generating double-stranded DNA breaks [32]. CRISPRi relies on a catalytically dead Cas9 (dCAS9) fused to a repressor domain, which, when guided by a sgRNA targeted to a particular promoter, results in the recruitment of endogenous modulators that lead to epigenetic modifications and subsequently gene knockdown [33–36].

We therefore envision that a strategy to query epistatic relationships acutely and systematically at scale, compatible with the sensitive phenotypic read-out afforded by a fluorescent reporter, would be a powerful tool for assigning genetic function. Towards this goal, we coupled existing CRISPRi technology with a simple and flexible dual-sgRNA library design that is compatible with multicolor FACS-based reporter screens. Our library design, which acutely delivers both a genetic 'anchor point' guide and a second randomized guide in a single plasmid, allows us to perform genetic modifier screens for essential and non-essential genes on a genome-wide scale. As a proof of principle, we applied this approach to dissecting the complex parallel pathways that mediate tail-anchored protein insertion into the endoplasmic reticulum (ER). This approach will be broadly applicable for (i) identifying functional redundancy, (ii) assigning factors to parallel or related biological pathways, and (iii) systematically reveal genetic interactions on a genome-wide scale for a given biological process.

Results

Dual sgRNA library design and construction

We developed a strategy to construct and deliver a library containing a fixed pre-determined guide, our genetic anchor point, with a second randomized CRISPRi guide from a single lentiviral backbone at scale (Fig. 1A). The basis of our second guide is the CRISPRi-v2 library, a compact, validated 5 sgRNA per gene library targeting protein-coding genes in the human genome [35]. Ease of use was a primary focus of the library design which we addressed by (i) ensuring library construction relied on straightforward and inexpensive restriction enzyme cloning, (ii) developing a sequencing strategy that serves as a failsafe to ensure both guides are present, eliminating potential background, and (iii) designing the library such that the resulting data could be analyzed using an existing computational pipeline.

A necessary requirement of our library design is identification of a pre-verified sgRNA that efficiently targets and depletes your gene of interest. This guide is first introduced by standard restriction enzyme cloning into a human U6 (hU6) and constant region 3 protospacer (CR3), hU6-CR3 cassette using sgRNA DNA oligos that can be inexpensively synthesized and purchased (Fig. 1B). Using complementary restriction enzyme sites, the resulting hU6-CR3 cassette is ligated into the CRISPRi-v2 library at scale, resulting in an mU6-CR1-hU6-CR3 guide design [31, 37]. As in the single element CRISPRi-v2 library, BFP and puromycin resistance genes are constitutively expressed, acting as fluorescent and selectable markers to identify guide-containing cells.

Sequencing of the resulting library couples standard barcoded 5' CRISPRi-v2 index primers with a new reverse primer complementary to the hU6 region, thereby only amplifying vectors containing the fixed sgRNA insert. This is important because during library construction, it is possible to produce a small fraction (we estimate < 2%) that lack the fixed guide. Additionally, because this cloning strategy involves restriction enzyme digest of the CRISPRi-v2 library, there is loss of a small number of guides that contain these cut sites (~1%, see Supplementary Table 1).

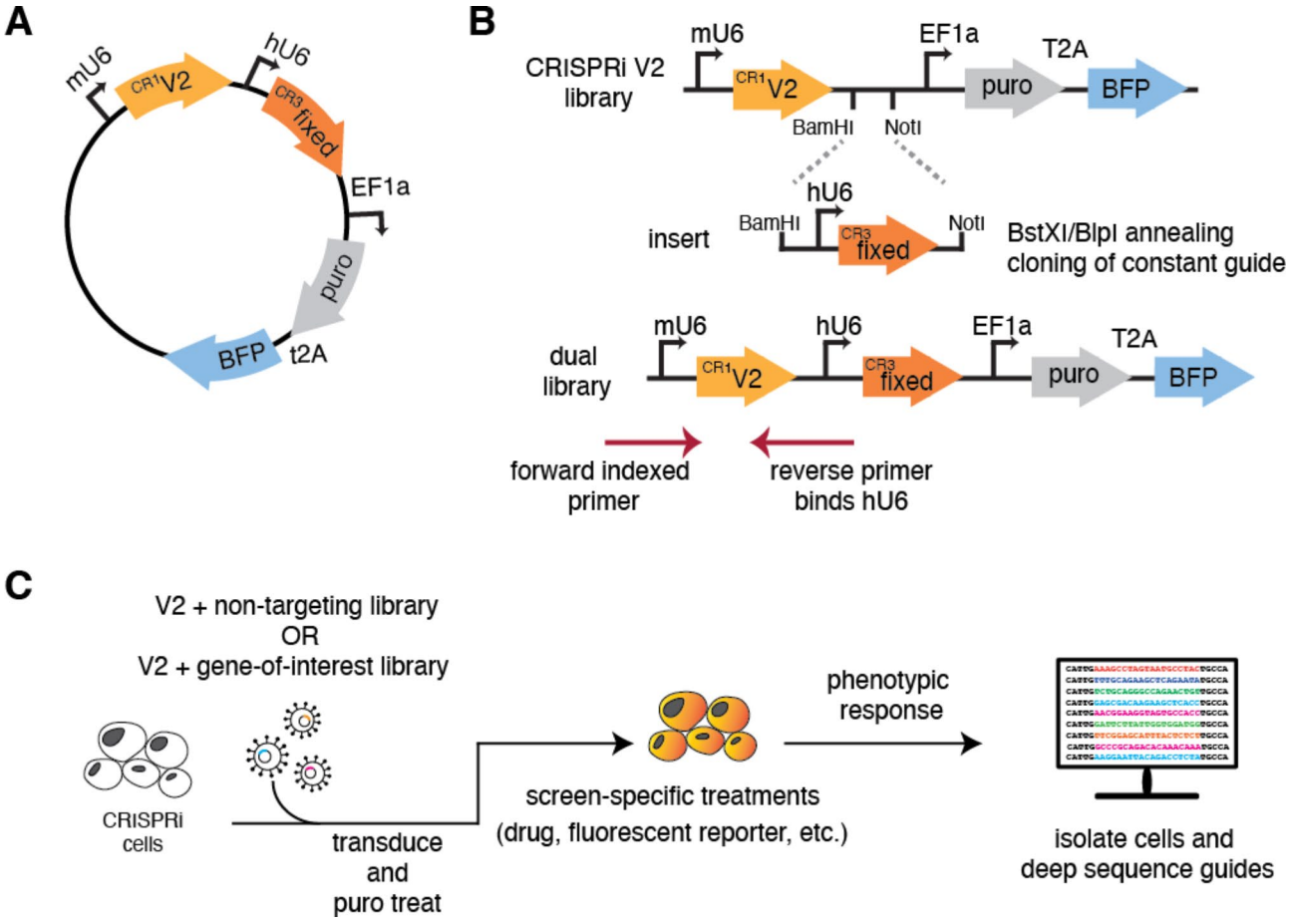

Fig. 1 Dual-guide library design and construction. **(A)** Schematic of the dual sgRNA vector. Expression of the randomized CRISPRi-v2 sgRNA is driven by a mU6 promoter and the fixed guide is driven by a hU6 promoter, each flanked by unique guide constant regions (CR). Downstream, the EF1a promoter drives the expression of the puromycin resistance selectable marker and BFP. **(B)** Cloning a dual genome-wide library is comprised of two steps. First, a guide of interest is inserted using standard oligo annealing and ligation into a BstXI/BlpI cut backbone. Second, both CRISPRi-v2 library and the fixed guide are digested with complementary restriction sites (BamHI/NotI) and ligated at scale, resulting in an mU6-'V2 guide'-hU6-'fixed guide' library design. To sequence the resulting library, a standard 5' indexed primer is coupled with a reverse primer that anneals to the hU6 region upstream of the inserted fixed guide. This strategy ensures only guides containing the fixed region are amplified for sequencing. **(C)** A general workflow for using our library design in any CRISPRi machinery containing cell

Putative use of this dual sgRNA library for genetic modifier screening

To test this procedure, we first generated a library with a verified 'non-targeting' sequence as the fixed guide. Comparison with the standard CRISPRi-v2 library shows that we maintain similar guide coverage across the genome after accounting for expected loss of the restriction site containing guides (Figure S1A) [35]. The resulting sgRNA library allows for the acute knockdown of two separate targets without the need for additional selection markers, which simplifies both growth screens and the more sensitive fluorescent reporter-based flow cytometry screens. This design also removes the need to first make a cell line constitutively expressing a targeting or non-targeting sgRNA, thereby ensuring both the gene-of-interest and the genome-wide library are knocked down for the same period of time, diminishing the possibility of adaptation. Our library design is therefore compatible with a workflow that permits querying epistatic relationships with a variety of phenotypic readouts in any cells expressing the CRISPRi machinery (Fig. 1C).

To test for genetic interactors at scale, one would conduct a screen using both the non-targeting library we have generated (available from Addgene, Library #197348), and a second library targeting a validated genetic 'anchor point' for your pathway of interest. Comparison of the results of these two screens, in the presence or absence of a characterized pathway component, will uncover and place factors in their respective pathway. We expect three possibilities. (i) Enhanced phenotypes in the 'anchor point' screen suggest synthetic effects, which would be indicative of factors in a parallel pathway, or a 'synergistic' effect. (ii) In contrast, diminished phenotypes in the anchor point screen would suggest factors in

the same pathway. (iii) Finally, factors with phenotypes independent of our genetic 'anchor point' likely represent orthogonal genes.

Developing a reporter assay to assess tail-anchored (TA) protein insertion at the endoplasmic reticulum (ER)

As a proof of principle, we tested the utility of our dual library by interrogating genetic interactors using a biological system known to contain at least two partially redundant pathways: tail-anchored membrane protein biogenesis. Tail anchored proteins (TAs) carry out essential functions including vesicle trafficking, organelle biogenesis, and cell-to-cell communication [38]. This family of integral membrane proteins are characterized by a single transmembrane domain (TMD) within 30–50 amino acids of their C terminus [39]. The proximity of the TMD to the stop codon necessitates that TAs be targeted and inserted into the membrane post-translationally. Though found in all cellular membranes, the majority of TAs are targeted to the ER using two parallel pathways: the Guided Entry of Tail-anchored protein (GET) and ER membrane protein complex (EMC) pathways [38, 40–42].

In mammalian cells, the central components of the GET system are the targeting factor GET3, and the ER resident insertase composed of the heterooligomeric GET1/GET2 complex [43, 44]. The EMC pathway relies on targeting by the cytosolic chaperone, Calmodulin to the nine-subunit EMC insertase [42]. The dependency of a particular TA on either set of factors is determined by the hydrophobicity of its TMD, with more hydrophobic substrates relying on the GET, and less hydrophobic substrates relying on the EMC [42, 45–47]. However, TAs of intermediate hydrophobicity can utilize both pathways for targeting and insertion into the ER, potentially obscuring genetic relationships [42]. We therefore reasoned that our dual-guide screening platform would be ideally suited to identify epistatic relationships between factors in these two pathways (Fig. 2A).

To assess TA biogenesis using a FACS-based approach, we adapted a fluorescent split GFP reporter system to specifically query insertion into the ER (Fig. 2B). For our reporter substrate, we chose SEC61β, which is an ER-localized TA that normally forms part of the heterotrimeric Sec61 translocation channel (along with Sec61α, and γ) [2, 48–50]. SEC61β contains a TMD of intermediate hydrophobicity and is known to use both the EMC and GET pathways for biogenesis [42]. We constitutively expressed the first 10 β-strands of GFP (GFP1-10) in the ER lumen and appended the 11th β-strand onto the C-terminal of the endogenous sequence of SEC61β (SEC61β-GFP11) [51, 52]. Successful insertion of SEC61β into the ER membrane would therefore result in complementation (GFP11+GFP1-10) and GFP fluorescence. To generate cell lines compatible for screening, we engineered K562 cells to stably express ER GFP1-10 and the dCas9-KRAB(Kox1) CRISPRi machinery. Under an inducible promoter, we integrated the SEC61β-GFP11 reporter alongside a normalization marker (RFP) separated by a viral 2A sequence (Figure S1B). Expression of both the TA and RFP from the same open reading frame allows us to use the GFP:RFP ratio to identify factors involved in TA biogenesis while discriminating against those that have a non-specific effect on protein expression levels (i.e. transcription or translation).

Interrogating TA insertion into the ER using dual sgRNA libraries

To permit screening with our dual-guide library design, we constructed a library using a previously validated EMC2 sgRNA as our 'fixed' guide (Figure S1C; Addgene Library #197349). EMC2 is a core, soluble subunit of the EMC, whose depletion leads to the post-translational degradation of the entire EMC via the ubiquitin-proteasome system [53, 54]. Therefore, targeting EMC2 is sufficient to disrupt the EMC pathway for TA insertion, and serves as our 'genetic anchor'. Using our reporter cell line, we confirmed using programmed dual guides that loss of both the EMC and GET2 resulted in a synergistic effect on SEC61β insertion (Fig. 2C). The enhanced effect of loss of GET2 in an EMC knockdown background validate the conceptual premise of our dual-guide screening approach at scale.

We therefore separately used both the EMC2 and a NT control library to transduce our K562 SEC61β reporter cell line, isolated cells that had perturbed GFP:RFP ratios by FACS, and identified the associated guides by deep sequencing. In parallel for comparison, we conducted a traditional growth screen with both the NT and EMC2 libraries in uninduced K562 SEC61β-GFP11 reporter cell lines (Figure S2A, Supplementary Table 2). As expected, in the NT-FACS screen loss of GET pathway components (GET2, GET3, and GET1) and all EMC subunits led to decreased SEC61β-GFP fluorescence, consistent with their established role in TA biogenesis. However, the EMC2-FACS screen showed markedly different results indicative of the genetic relationships between the EMC and GET pathway components (Fig. 3A). First, when depleted on top of EMC2, the phenotype effects of loss of the main GET pathway factors is enhanced when compared to the NT screen. Second, the majority of guides targeting EMC subunits no longer have significant effects on SEC61β-GFP, consistent with being in the same complex, and therefore same pathway, as EMC2 [53, 54]. The exceptions are EMC2 itself, likely because two guides targeting the same gene leads to a greater degree of knockdown, and EMC10, which has been suggested to have a separate regulatory role in TA biogenesis [55]. Conversely, in both screens we also identified

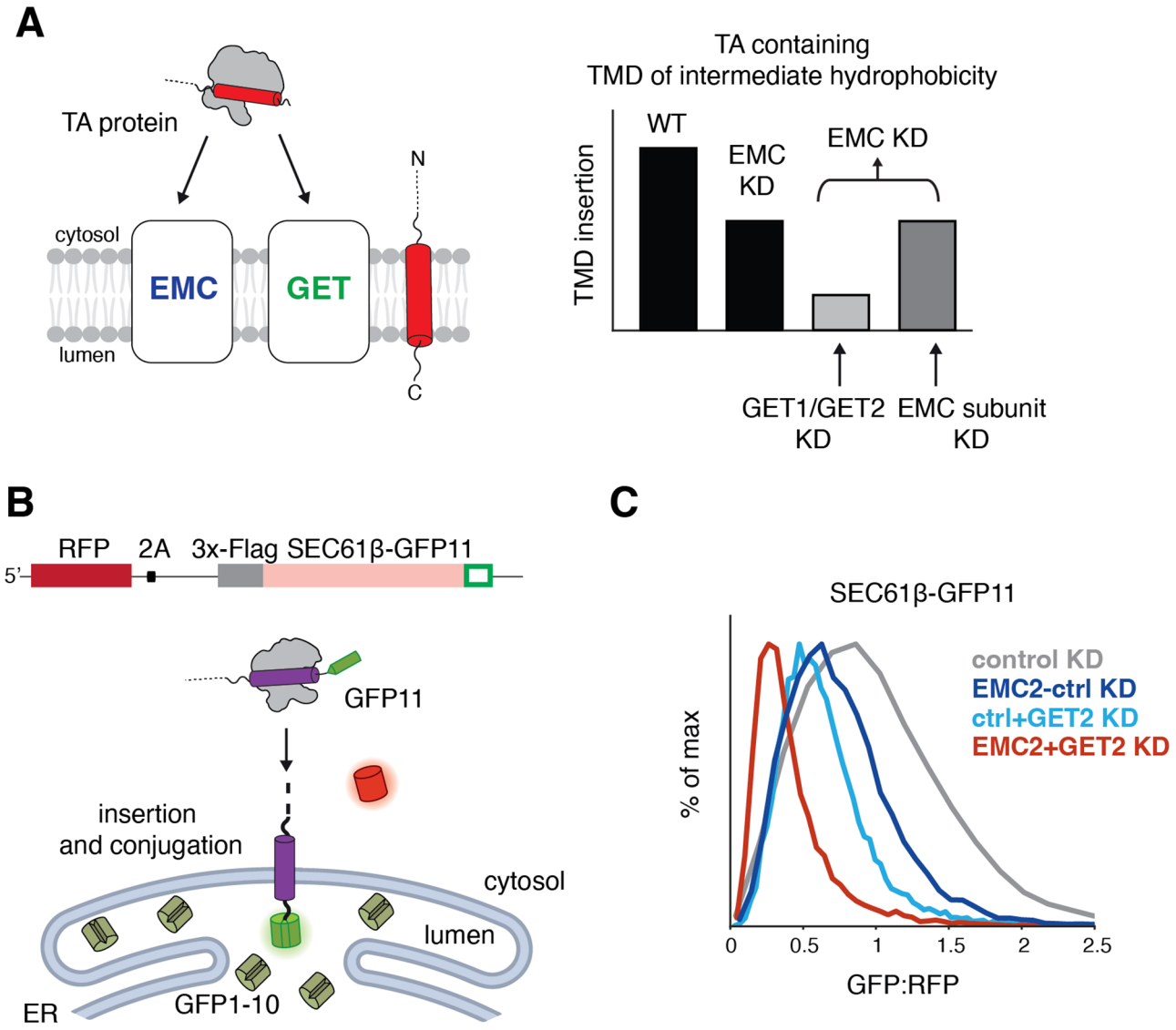

Fig. 2 Querying tail-anchored (TA) protein biogenesis at the endoplasmic reticulum (ER). **(A)** (Left) TA proteins can be inserted into the lipid bilayer by either the EMC or GET insertases. (Right) TAs containing a moderately hydrophobic transmembrane domain such as SEC61β can use either EMC or GET1/GET2 to insert, obscuring strong effects on insertion when obstructing only one of these partially redundant pathways. Therefore, use of an EMC2 fixed guide dual library should uncover defined epistatic relationships between factors in either the GET or EMC pathways. **(B)** Schematic of the split GFP reporter system used to assess insertion of SEC61β into the ER. K562 cells expressing CRISPRi machinery were engineered to constitutively express GFP1-10 in the ER lumen. The 11th β -strand of GFP is fused to the C-terminus of SEC61β, allowing for conjugation and fluorescence of the full GFP upon insertion into the ER membrane. RFP is expressed as a normalization marker, separated by a viral P2A sequence. **(C)** Depletion of EMC and GET pathway components in the SEC61β reporter cell line. The SEC61β cell line was separately transduced with dual guides targeting EMC2 alone, GET2 alone, EMC2 and GET2, or a non-targeting control. The GFP:RFP ratio, a measure of SEC61β insertion at the ER, is plotted for each dual guide

several novel ER-resident factors (RNF185, TMEM259 and FAF2) whose depletion leads to increased stability of SEC61β-GFP. Presumably, these putative quality control factors are responsible for recognizing and degrading over-expressed SEC61β from the membrane, but are agnostic to which biogenesis pathway was initially used for its insertion.

To facilitate comparison of screens for identification of genetic interactors, we calculated a discriminant score for each gene, which integrates the statistical confidence and phenotype into a single value, as previously described [56]. A similar strategy is routinely used to categorize statistically significant from non-significant hits when analyzing genome-wide screens using volcano plots [35]. Genes are further ranked by their discriminant scores and the change in rank between the two screens is calculated. This allowed us to visualize the effects of a specific gene on SEC61β stability in the absence or presence of EMC2 (Fig. 3B). Comparison of the NT- and EMC2-genome-wide FACS screens using the discriminant score

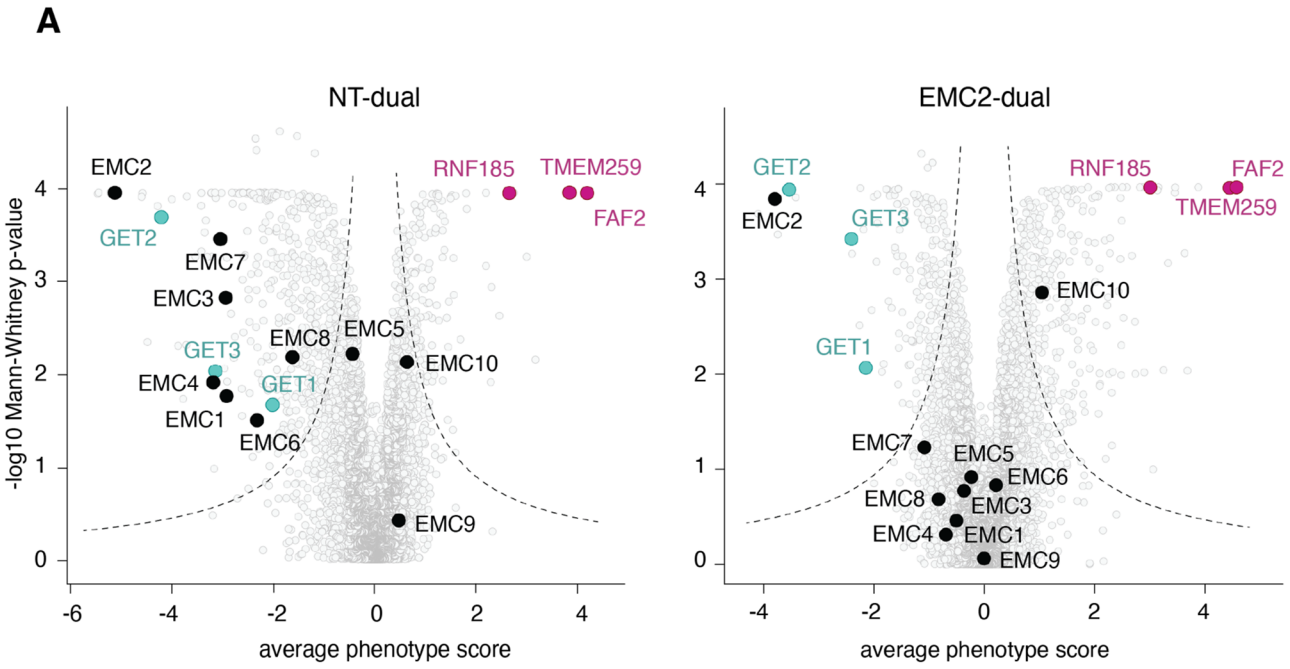

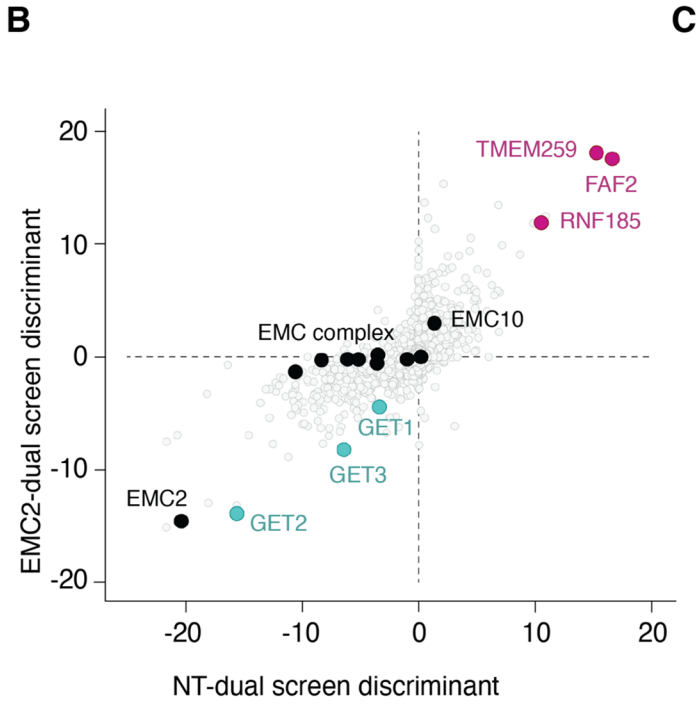

C

gene	NT	EMC2	Δ rank
GET2	9	3	6
GET3	105	7	98
GET1	266	47	219
EMC1	156	4072	-3916
EMC2	4	2	2
EMC3	62	3329	-3267
EMC4	120	4369	-4249
EMC5	852	4405	-3553
EMC6	249	34743	-34494
EMC7	30	317	-287
EMC8	242	1272	-1030
EMC10	40519	40565	-46

Fig. 3 Dual-guide CRISPRi screen with SEC61β reveals genetic interactions between GET and EMC pathway components. **(A)** Volcano plot illustrating the phenotype for the two strongest guide RNAs versus log10 (Mann-Whitney p-values) from two independent replicates of a genome-wide screen with either non-targeting dual (NT) or EMC2-dual libraries using the SEC61β-GFP11 reporter. Individual genes are displayed in gray, core factors of the GET pathway are highlighted in green, EMC subunits are highlighted in black, while putative stabilization factors are in pink. **(B)** A single discriminant score was computed for each gene in the screens investigating SEC61β-GFP11 stability, representative of the average phenotype score and significance of the hit in the respective screen. This metric allows direct comparison of both NT-dual and EMC2-dual screens. **(C)** Comparison of genes ranked by discriminant score in NT and EMC2-dual screens

highlighted the three broad categories of factors we anticipated: members of the GET pathway which show a synthetic effect with EMC, members of the EMC pathway which effectively 'drop out' in the absence of EMC2, and factors which operate orthogonally from both pathways and are therefore unchanged in the two conditions (Fig. 3C).

To confirm a subset of the observations predicted by our reporter-based screens, we conducted arrayed assays with programmed dual guides. Using our SEC61β-GFP11 reporter, we show that depletion of both EMC2 and GET3 has an enhanced effect on biogenesis compared to obstructing either pathway individually. This effect is likely specific to substrates of intermediate TMD hydrophobicity, as squalene synthase (SQS), a TA with known EMC dependency is only affected in the absence of EMC2 (Fig. 4A) [53]. Additionally, depletion of the putative quality control components RNF185, TMEM259 or FAF2 have affects the stability of SEC61β (Fig. 4B), but not SQS or the GET substrate VAMP (Figure S3A). Indeed, RNF185 and TEMEM259 have been recently identified as members of a novel arm of ER-associated degradation (ERAD), while FAF2 has been previously associated with ERAD [57–59].

To illustrate the efficacy of our strategy, we compared the results of our FACS-based dual-guide library screen to a more traditional growth screening approach. Using growth as the metric, there is no increased genetic reliance on GET pathway components in the absence of EMC2 (Figure S2B, Supplementary Table 3). This is consistent with the observation that a substantial number of genes with transcriptional phenotypes have negligible growth phenotypes [37]. The significant number of hits both in the presence and absence of EMC2 are essential genes, occluding the possibility of detecting significant factors in the context of a particular biological pathway (Figure S2C). Given these results, hits identified from the growth screening approach would be particularly prone to off-pathway false positive and false negatives, necessitating substantial more follow-up to identify bona fide genetic interactors of the EMC. If we assume no previous knowledge of the relationship between the EMC and GET pathways, the growth-based approach clearly fails to identify genetic interactions that are crucial to elucidating its biological function, thereby illustrating the efficacy and potential utility of our dual-guide screening approach.

Discussion

We have developed a flexible, straightforward strategy to rapidly assess genetic interactions genome-wide with high efficiency. Successful implementation of this approach does require sufficient prior knowledge of pathway or candidate gene of interest both to identify the fixed guide and design and validate an appropriate fluorescent reporter. However, the dual-guide strategy offers several practical advantages over existing genetic modifier screening strategies. Our approach eliminates the need to create and characterize a knockout line for a particular gene of interest [25, 29, 60–62]. It also allows for the simultaneous delivery and selection of both targeted and genome-wide elements, resulting in less cell line

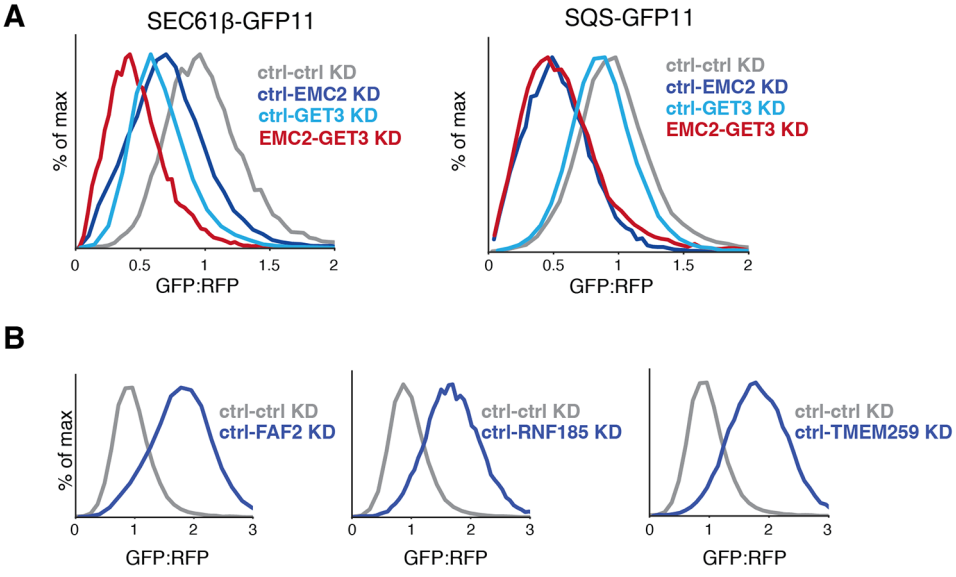

Fig. 4 Validating effects of factors on TA biogenesis. **(A)** Integration of the TA proteins SEC61β -GFP11 or SQS-GFP11 into the ER was assessed in K562 cells that expressed the indicated programmed dual guides. GFP fluorescence is shown relative to a normalization marker (RFP) as determined by flow cytometry, and the results displayed as a histogram. **(B)** Biogenesis of SEC61β-GFP11 was assessed as in (A) with the presence of guides targeting the indicated genetic targets

construction and manipulation. The dual-guide library approach is compatible with multiple screening modalities while allowing for genome-wide perturbations, notably flow cytometry-based approaches where number of fluorophores may be limited. Finally, construction and use of new libraries is easy and rapid, with a two-step cloning process and reliance on existing sequencing and analysis pipelines. However, one minor caveat of the dual-guide system is that the addition of a second guide delivered on the same plasmid diminishes the efficiency of the fixed guide, but not by a significant amount (Figure S3B-C). This is evident in our system, with EMC2 coming out as a significant hit in the EMC2-dual-guide reporter screen. This can be ameliorated by the selection of a fixed guide that independently results in efficient knockdown, and the use of the recently described Zim3-Cas9 effector system, which has been shown to have stronger on-target knockdown compared to KOX1-Cas9 while maintaining minimal non-specific genome-wide effects [63, 64].

Recent studies have highlighted the success of FACS-based CRISPRi screens for the discovery of new factors [52, 65–67]. Our library extends the use case of this approach, for example allowing the study of processes that have parallel compensatory pathways, such as protein biosynthesis and degradation. Though a single screen with a programmed guide containing dual library is sufficient for most applications, performing an additional screen with a NT guide-containing dual library provides additional data that could reveal critical genetic interactions. Another implication of our work is the relative paucity of information in traditional growth-based screens, with no additional perturbations. Moving forward, we propose that additional up-front investment in developing a more targeted phenotypic read out, whether it be sensitivity to a compound or a reporter, is worthwhile when trying to establish genome-wide genetic interactions.

Conclusion

The ability to genetically interrogate a biological process in mammalian cells on a genome-wide scale is a powerful tool to determine gene function. Here, we propose a simple advance to current CRISPRi sgRNA library construction that couples a genome-wide library with the simultaneous knockdown of a particular gene of interest. As a proof of principle, we use this design with a FACS-based reporter screen to show the relationships between the parallel pathways that mediate the insertion of TA proteins into the endoplasmic reticulum (ER). We not only faithfully reveal the known factors involved in this process, but can place them in either the GET or EMC pathways. We envision that these screening approaches represent a powerful strategy to unbiased and systematic identification of genetic interactors, capable of de-orphaning genes of interest.

Materials and methods

Plasmids

Sequences used for in vivo analysis were derived from UniProtKB/Swiss-Prot and included: squalene synthase isoform 1 (SQS/FDFT1; **Q6IAX1**), vesicle associated membrane protein 2 (VAMP; **P51809-1**), and SEC61β (SEC61B, NP_006799.1). For expression in K562 cells, the transmembrane domain (TMD) and flanking regions of respective ER localized proteins were inserted into a backbone containing a UCOE-EF-1α promoter and a 3′ WPRE element (Addgene #135448) [68]. The exception was the SEC61β construct used for the CRISPRi screens (RFP-P2A-Sec61b-GFP11) which was integrated into an SFFV-tet3G backbone [68]. The GFP:RFP reporter system has previously been described [42, 69] and used in the context of CRISPRi screens [52]. The mCherry variant of RFP was used in all constructs, but is referred to as RFP throughout the text and figures for simplicity. For VAMP2, SQS and SEC61β, directly upstream of the TMD and flanking regions, the first 70 residues of the flexible cytosolic domain of SEC61β was inserted. Downstream, the GFP11 tag (RDHMVLHEYVNAAGIT) was inserted at the C-terminal separated by a 2-4X GS linker to allow for complementation with GFP1-10. In order to express GFP1-10 in the ER lumen, the human calreticulin signal sequence was appended preceding GFP1-10-KDEL as previously described [51, 70, 71].

Programmed dual sgRNA guide vectors were used to allow for the simultaneous depletion of genes [37]. Dual guide pairs included: EMC2-Control (GGAGTACGCGTCCGGGCCAA, GACGACTAGTTAGGCGTGTA), Control-GET2 (GACGACTAGTTAGGCGTGTA, GATGTTGGCCGCCGCTGCGA), EMC2-GET2 (GGAGTACGCGTCCGGGCCAA, GATGTTGGCCGCCGCTGCGA), Control-Control (GACGACTAGTTAGGCGTGTA, GACGACTAGTTAGGCGTGTA), Control-GET3 (GACGACTAGTTAGGCGTGTA, GGCTCCAGCGGCTCCACATC), EMC2-GET3 (GGAGTACGCGTCCGGGCCAA, GGCTCCAGCGGCTCCACATC), Control-FAF2 (GACGACTAGTTAGGCGTGTA, GCGGGTCAGGAGCGTAGAGG), Control-RNF185 (GACGACTAGTTAGGCGTGTA, GGCTGGCGTTAACTGTGCGG), Control-TMEM259 (GACGACTAGTTAGGCGTGTA, GCGGACGAGAAAGCGGAAGA). All reporter constructs and programmed dual guides are available upon request.

pCMV-VSV-G was a gift from Bob Weinberg (Addgene plasmid # 8454 ; http://n2t.net/addgene:8454 ; RRID:Addgene_8454).

CRISPRi dual-guide library construction

Following selection and verification of a fixed guide, it is cloned into a hU6-CR3 cassette flanked by BamHI/NotI restriction cut sites (pJR152, Addgene #196280). The pJR152 backbone is compatible with standard BstXI/BlpI ligation with annealed oligos. Guide oligos must be ordered with custom overhangs (forward oligo: "ATG"-guide sequence-"GTTTCAGAGC"; reverse oligo: "TTAGCTCTGAAAC" – reverse complement of guide sequence – "CATGTTT"). For the NT and EMC2 libraries, the fixed guides were "GACGACTAGTTAGGCGTGTA" and "GGAGTACGCGTCCGGGCCAA", respectively.

The two components of the dual-guide library are pJR152 containing the fixed guide of interest, and the CRISPRi-v2 library (Addgene Pooled Libraries #83969) [35] (https://www.addgene.org/pooled-library/weissman-human-crispri-v2/). Construction of the dual-guide library essentially consists of restriction digesting both elements with BamHI/NotI and inserting the hU6-CR3-fixed guide element into the CRISPRi-v2 library at scale, resulting in an mU6-CR1-hU6-CR3 design previously described [72].

Specifically, the pJR152 containing either the NT or EMC2 targeting guide was restriction digested at 37 C for 3 h with BamHI/NotI, and the resulting 400 bp gene fragment (containing the hU6-CR3-fixed guide element) gel purified. Approximately 30 µg of the CRISPRi-v2 top5 library was restriction digested with BamHI/NotI in the presence of shrimp alkaline phosphatase (rSAP) for 6 h at 37 C followed by heat inactivation at 65 C for 5 min. Smaller amounts of the CRISPRi-v2 library can be digested, but a larger initial reaction will prevent repeat digestions and subsequent quality control checks. Ensure that no more than 10% of the reaction is enzyme to prevent star activity or inactivation of restriction enzymes. The resulting fragment of 8,800 base pairs was gel purified and eluted in a smaller volume. Following recovery of both elements, either NT of EMC2 guide containing inserts were T4 ligated (ensure it is NEB #M0202M) with an insert to vector ratio of 1:2 for 16 h at 16 C. Various vector:insert molar ratios were tested during piloting, with 1:2 resulting in the highest efficiency. A control ligation containing just the restriction digested CRISPRi-v2 library should be included.

To assess background, a small amount (0.5 µL of 20 µL) of the resulting ligations as well as the control were transformed into 10 µL of Stellar chemically competent cells (Takara #636,763) using manufacturer guidelines. Various dilutions were plated (1/10th, 1/100th, and 1/1000th) with the resulting colonies counted on both control plates and dual library plates. Successful digestion and ligation should result in <2% background colonies, with the concern that single guides may pack much better than dual guides into lenti-virus, and therefore be over-represented.

To permit electrophoresis into MegaX cells at scale (ThermoFisher #C640003) the rest of the dual T4 library ligation for either NT or EMC2 dual libraries is selected with SPRISelect beads (Beckman Coulter B23317) and eluted in 20 µL of water. The entire resulting elution were electroporated into MegaX cells using manufacturer guidelines. Electroporated cells are allowed to recover and set up in an overnight culture of 200 mL LB supplemented with 100 µg/mL carbenicillin for each library. A smaller proportion of the culture was taken (1/1,000th and 1/10,000th) and plated to allow for the estimate of resulting colonies and therefore guide coverage, with the expectation of maintaining 50X coverage for the 100,000 element CRISPRi-v2 library. Resulting NT and EMC2 dual libraries were amplified and barcoded by PCR using NEB Next Ultra ii Q5 MM (M0544L) and index primers and a unique reverse primer (CAAGCAGAAGACGGCATACGAGATggaatcatgggaaataggccctc) that binds in the hU6 region upstream of the fixed guide. The standard CRISPRi-v2 library was amplified in parallel to allow for the assessment of guide representation in dual libraries [35]. SPRISelect beads (Beckman Coulter B23317) were used to purify the dual DNA libraries (349 bp), and purified DNA was sequenced using an Illumina HiSeq2500 with the same sequencing primer as the standard CRISPRi-v2 library (GTGTGTTTTGAGACTATAAGTATCCCTTGGAGAACCACCTTGTTG). The NT and EMC2 dual libraries are available on Addgene (Library #197348 and Library #197349, respectively).

Cell culture and cell line construction

Cells	Source
K562 KRAB-BFP-dCAS9	Gilbert et al., 2014 [34]
HEK 293T/17	ATCC CRL-11,268
K562 KRAB-BFP-dCAS9 ER GFP1-10	Guna et al., 2022 [52]
K562-CRISPRi-Tet-ON-((ER)-GFP1-10)-(tet-RFP-P2A-SEC61β-GFP11)	This study, available upon request

K562 cells expressing KRAB-BFP-dCas9 [34] were cultured in RPMI-1640 with 25 mM HEPES, 2.0 g/L $NaHCO_3$, and 0.3 g/L L- glutamine supplemented with 10% FBS (or Tet System Approved FBS), 2 mM glutamine, 100 units/mL penicillin, and 100 µg/mL streptomycin. Cells were maintained between 0.25×10^6 -1×10^6 cells/mL. HEK293T/17 (ATCC CRL-11,268) cells were cultured in DMEM supplemented with 100 units/mL penicillin and 100 µg/mL streptomycin. K562 and HEK293T cells were grown at 37 C.

Cell lines expressing GFP1-10 in the ER lumen were generated as previously described [51, 52]. CRISPRi K562 cells were infected with lenti virus containing CalR(GFP1-10)-KDEL and sorted with a Sony Cell Sorter

(SH800S) as single clones into 96-well plates. Clones were expanded and confirmed by complementation with a construct targeted to the ER appended to GFP11. To generate the SEC61β line used for screening line, lentivirus containing ER(GFP1-10) and RFP-P2A-SEC61β-GFP11 under an inducible promoter were co-infected at one copy per cell line in CRISPRi (expressing KRAB-BFP-dCas9) K562 Tet-ON cells [34]. Cells were then single cell sorted, verified by induction with doxycycline (100 ng/μL), and confirmed to localize to the ER by microscopy. These cells are referred to as K562-CRISPRi-Tet-ON-((ER)-GFP1-10)-(tet-RFP-P2A-SEC61β-GFP11).

Lentivirus production

Lentivirus was generated using standard protocols. Briefly, HEK293T cells were co-transfected with two packaging plasmids (pCMV-VSV-G and delta8.9, Addgene #8454) and either a desired transfer plasmid, or the dual libraries, using Transit-IT-293 transfection reagent (Mirus) [73]. Approximately 48 h after transfection, the supernatant was collected and flash frozen. Virus was rapidly thawed at 37 C prior to transfection.

Flow cytometry reporter CRISPRi screens

CRISPRi screens were performed as previously described, with minor modifications [34, 35]. Either the NT or EMC2 dual libraries were transduced in duplicate into 330 million K562-CRISPRi-Tet-ON-((ER)-GFP1-10)-(tet-RFP-P2A-Sec61b-GFP11) cells at a multiplicity of infection less than one. Throughout the screen, cells were maintained in 1 L spinner flasks (Bellco, SKU: 1965–61,010) at a volume of 1 L. 48 h after transfection, BFP positive cells were between 30 and 35%. At this point, cells began treatment with 1 μg/mL puromycin for three days to select for guide positive cells. Cells were given two days to recover after puromycin selection and the reporter was induced with doxycycline (100 ng/mL) for 24 h and sorted on a FACSAria Fusion Cell Sorter. Cells were daily diluted to 0.5×10^6 cells/mL to ensure that the culture was maintained at an average coverage of more than 1000 per sgRNA.

During sorting, cells were gated for BFP (to select only guide-positive cells) and RFP and GFP (indicating an expressing reporter). Cells were sorted based on the GFP:RFP ratio of the final gated population, and roughly 40 million cells with either the highest or lowest 30% GFP:RFP ratios were collected, pelleted, and flash-frozen. Genomic DNA of the cell pellets was extracted and purified using a Nucleospin Blood XL kit (Takara Bio, #740950.10). Guides were amplified and barcoded by PCR using NEB Next Ultra ii Q5 MM (M0544L) and index primers and a unique reverse primer (CAAGCAGAAGACGGCATACGAGATggaatcatgggaaataggccctc) that binds in the hU6 region upstream of the fixed guide. This ensures that only DNA containing both the v2 library and one of the fixed EMC2 or NT guides is amplified and sequenced. SPRISelect beads (Beckman Coulter B23317) were used to purify the DNA library (349 bp), and purified DNA was analyzed on an Agilent 2100 Bioanalyzer prior to sequencing using an Illumina HiSeq2500 using the same sequencing primer as the standard CRISPRi-v2 library (GTGTGTTTTGAGACTATAAGTATCCCTTGGAGAACCACCTTGTTG). Post-sequencing analysis was performed using the pipeline in https://github.com/mhorlbeck/ScreenProcessing [35]. Guides with fewer than 50 counts were excluded to ensure proper coverage. For each screen, the strongest 3 sgRNA phenotypes were used to calculate the phenotype score of each gene. The Mann-Whitney p-value was calculated using all 5 sgRNAs targeting the same gene compared to negative controls (Supplementary Table 2). Since screens were performed in biological duplicate, the sgRNA phenotypes were averaged. Discriminant scores were calculated as the product of the gene's phenotype score and the Mann-Whitney p-value. Discriminant ranks for each screen were determined by ranking the list of genes from lowest to highest discriminant values, with the lowest score the highest rank.

CRISPRi growth screens

To perform the growth screen, the same cells for flow cytometry screens infected with either NT or EMC2 dual libraries were harvested after recovery from puromycin selection as Day 0, and then again after 10 doublings on Day 18. 50 million cells from each biological duplicate and each library were harvested. Cells were maintained at an average coverage of more than 1000 per sgRNA during all points of the growth screen, and >99% BFP positive cells were confirmed at the time of harvesting. Resulting libraries were extracted, amplified, purified and sequenced identically as for the flow-cytometry based screen samples as described above (Supplementary Table 3).

Flow cytometry

For all reporter assays, K562 CRISPRi cells containing ER(GFP1-10) were spinfected with lentivirus of indicated guides and knockdown was allowed for 6 days. Cells were then spinfected with lentivirus containing the indicated reporters and analyzed by flow cytometry after 48–72 h. All reporter experiments were performed in biological triplicate. All samples were either run on an NXT Flow Cytometer (ThermoFisher) or a MACSQuant VYB (Miltenyi Biotec). Flow cytometry data was analyzed either in FlowJo v10.8 Software (BD Life Sciences) or Python using the FlowCytometryTools package.

Quantitative PCR

Quantitative PCR was used to analyze RNA levels after knockdown with dual or single guides. K562

cells expressing the CRISPRi machinery were infected with guides and after 8 days of knockdown, RNA was extracted and treated with DNaseI using a Direct-zol RNA MiniPrep Plus kit (R2072, Zymo). Purified RNA was reverse transcribed using the SuperScript III First-Strand Synthesis SuperMix for qRT-PCR kit (11,752,050, Invitrogen). Reactions were run on a StepOnePlus Real-Time PCR system and knockdown efficiency was calculated using the housekeeping gene HPRT1. Samples were collected and analyzed in triplicate with the means and standard deviations plotted. The primers used were: EMC2 (fwd AGACAGTTCCCTGGCAGTCAC, rev TCCACATTTTTCCCCTGGGCT); GET2 (fwd CCGGATCATGGGCTTTCACA, rev CCTGCTGGTCAGTTGTTCCT).

Supplementary Information

The online version contains supplementary material available at https://doi.org/10.1186/s12864-023-09754-y.

Supplementary Material 1

Supplementary Material 2

Supplementary Material 3

Supplementary Material 4

Acknowledgements

We thank K. Hickey, R. Saunders, K. Popova and A. Inglis for helpful discussions. We thank the Whitehead Institute Flow Cytometry Core access to FACS machines and flow cytometers, and the Millard and Muriel Jacobs Genetics and Genomics Laboratory at Caltech for sequencing of screening libraries.

Authors' contributions

K.P., A.G. J.R. and R.M.V. were responsible for conceptual design of the project. K.P., A.G., T.E., and M.W. performed experiments, K.P. and A.G. performed data analysis, and K.P., A.G., and R.M.V wrote the manuscript. R.M.V. and J.S.W. provided funding. All authors read and approved the final manuscript.

Funding

Research reported in this publication was supported by: Howard Hughes Medical Institute (JSW), Center for Genome Editing and Recording 2RM1 HG009490-06 (JSW), Human Frontier Science Program 2019 L/LT000858 (AG), the Heritage Medical Research Institute (RMV), the NIH's National Institute of General Medical Sciences (DP2GM137412) (RMV), the Sontag Foundation (RMV), the Burroughs Wellcome Pathogenesis Investigator Program (RMV), NIH F31 Ruth L. Kirchstein National Research Service Award NS115380 (JMR), Rosen Family fellowship (KRP), and Arie Jan Haagen-Smit Fellowship (KRP).

Data availability

All materials necessary for dual-guide construction are available via Addgene, with accession numbers listed in the Materials and Methods. All programmed sgRNA, reporter constructs and cell lines are available from the corresponding author upon request. The sequencing datasets generated during the current study are available in the Caltech DATA repository and can be publicly accessed, https://doi.org/10.22002/3hvyj-yzq30.

Declarations

Ethics approval and consent to participate

Not applicable.

Consent for publication

Not applicable.

Competing interests

JMR consults for Maze Therapeutics and Waypoint Bio. JSW declares outside interest in 5 AM Venture, Amgen, Chroma Medicine, KSQ Therapeutics, Maze Therapeutics, Tenaya Therapeutics, Tessera Therapeutics, and Third Rock Ventures. RMV is a consultant and equity holder in Gate Bioscience. The Regents of the University of California with JSW as inventor have filed patent applications related to CRISPRi/a screening and Perturb-seq. JSW is an inventor on US Patent 11,254,933 related to CRISPRi/a screening. No potential conflicts of interests were declared by the other authors.

Received: 20 June 2023 / Accepted: 19 October 2023
Published online: 30 October 2023

References

1. Badano JL, Katsanis N. Beyond Mendel: an evolving view of human genetic Disease transmission. Nat Rev Genet. 2002;3:779–89.
2. Hartmann E, Sommer T, Prehn S, Görlich D, Jentsch S, Rapoport TA. Evolutionary conservation of components of the protein translocation complex. Nature. 1994;367:654–7.
3. Morishima Y, Wang AM, Yu Z, Pratt WB, Osawa Y, Lieberman AP. CHIP deletion reveals functional redundancy of E3 ligases in promoting degradation of both signaling proteins and expanded glutamine proteins. Hum Mol Genet. 2008;17:3942–52.
4. Itakura E, Zavodszky E, Shao S, Wohlever ML, Keenan RJ, Hegde RS. Ubiquilins Chaperone and Triage Mitochondrial Membrane Proteins for degradation. Mol Cell. 2016;63:21–33.
5. Rodina A, Wang T, Yan P, Gomes ED, Dunphy MP, Pillarsetty N, et al. The epichaperome is an integrated chaperome network that facilitates tumour survival. Nature. 2016;538:397–401.
6. Rutherford SL, Lindquist S. Hsp90 as a capacitor for morphological evolution. Nature. 1998;396:336–42.
7. Lehner B, Crombie C, Tischler J, Fortunato A, Fraser AG. Systematic mapping of genetic interactions in Caenorhabditis elegans identifies common modifiers of diverse signaling pathways. Nat Genet. 2006;38:896–903.
8. Costanzo M, Baryshnikova A, Bellay J, Kim Y, Spear ED, Sevier CS, et al. The genetic landscape of a cell. Science. 2010;327:425–31.
9. Tsherniak A, Vazquez F, Montgomery PG, Weir BA, Kryukov G, Cowley GS, et al. Defining a cancer dependency map. Cell. 2017;170:564–76. e16.
10. Behan FM, Iorio F, Picco G, Gonçalves E, Beaver CM, Migliardi G, et al. Prioritization of cancer therapeutic targets using CRISPR–Cas9 screens. Nature. 2019;568:511–6.
11. Winzeler EA, Shoemaker DD, Astromoff A, Liang H, Anderson K, Andre B, et al. Functional characterization of the S. Cerevisiae genome by gene deletion and parallel analysis. Science. 1999;285:901–6.
12. Eshed Y, Baum SF, Perea JV, Bowman JL. Establishment of polarity in lateral organs of plants. Curr Biol. 2001;11:1251–60.
13. Eshed Y, Baum SF, Bowman JL. Distinct mechanisms promote polarity establishment in carpels of Arabidopsis. Cell. 1999;99:199–209.
14. Ding Y, Long PA, Bos JM, Shih Y-H, Ma X, Sundsbak RS, et al. A modifier screen identifies DNAJB6 as a cardiomyopathy susceptibility gene. JCI Insight. 2016;1:e88797.
15. Hannan SB, Dräger NM, Rasse TM, Voigt A, Jahn TR. Cellular and molecular modifier pathways in tauopathies: the big picture from screening invertebrate models. J Neurochem. 2016;137:12–25.
16. Ahmad ST, Sweeney ST, Lee JA, Sweeney NT, Gao FB. Genetic screen identifies serpin5 as a regulator of the toll pathway and CHMP2B toxicity associated with frontotemporal dementia. Proceedings of the National Academy of Sciences. 2009;106:12168–73.
17. Hurd TR, Leblanc MG, Jones LN, DeGennaro M, Lehmann R. Genetic modifier screens to identify components of a redox-regulated cell adhesion and migration pathway. Methods Enzymol. 2013;528:197–215.
18. Najm FJ, Strand C, Donovan KF, Hegde M, Sanson KR, Vaimberg EW, et al. Orthologous CRISPR–Cas9 enzymes for combinatorial genetic screens. Nat Biotechnol. 2018;36:179–89.
19. Diehl V, Wegner M, Grumati P, Husnjak K, Schaubeck S, Gubas A, et al. Minimized combinatorial CRISPR screens identify genetic interactions in autophagy. Nucleic Acids Res. 2021;49:5684–704.

20. Wong AS, Choi GC, Cui CH, Pregernig G, Milani P, Adam M et al. Multiplexed barcoded CRISPR-Cas9 screening enabled by CombiGEM. Proceedings of the National Academy of Science. 2016;113:2544–9.
21. Soldner F, Laganière J, Cheng AW, Hockemeyer D, Gao Q, Alagappan R, et al. Generation of isogenic pluripotent stem cells differing exclusively at two early onset Parkinson point mutations. Cell. 2011;146:318–31.
22. Perreault N, Sackett SD, Katz JP, Furth EE, Kaestner KH. Foxl1 is a mesenchymal modifier of Min in carcinogenesis of stomach and colon. Genes Dev. 2005;19:311–5.
23. Johnston DS. The art and design of genetic screens: Drosophila melanogaster. Nat Rev Genet. 2002;3:176–88.
24. Zeng H, Castillo-Cabrera J, Manser M, Lu B, Yang Z, Strande V, et al. Genome-wide CRISPR screening reveals genetic modifiers of mutant EGFR dependence in human NSCLC. eLife. 2019;8:e50223.
25. Hickey KL, Dickson K, Cogan JZ, Replogle JM, Schoof M, D'Orazio KN, et al. GIGYF2 and 4EHP inhibit translation initiation of defective messenger RNAs to assist ribosome-associated quality control. Mol Cell. 2020;79:950–62. e6.
26. Kramer NJ, Haney MS, Morgens DW, Jovičić A, Couthouis J, Li A, et al. CRISPR–Cas9 screens in human cells and primary neurons identify modifiers of C9ORF72 dipeptide-repeat-protein toxicity. Nat Genet. 2018;50:603–12.
27. Chai N, Haney MS, Couthouis J, Morgens DW, Benjamin A, Wu K, et al. Genome-wide synthetic lethal CRISPR screen identifies FIS1 as a genetic interactor of ALS-linked C9ORF72. Brain Res. 2020;1728:146601.
28. DeWeirdt PC, Sangree AK, Hanna RE, Sanson KR, Hegde M, Strand C, et al. Genetic screens in isogenic mammalian cell lines without single cell cloning. Nat Commun. 2020;11:752.
29. Fu Y, Foden JA, Khayter C, Maeder ML, Reyon D, Joung JK, et al. High-frequency off-target mutagenesis induced by CRISPR-Cas nucleases in human cells. Nat Biotechnol. 2013;31:822–6.
30. Hsu PD, Lander ES, Zhang F. Development and applications of CRISPR-Cas9 for genome engineering. Cell. 2014;157:1262–78.
31. Norman TM, Horlbeck MA, Replogle JM, Ge AY, Xu A, Jost M, et al. Exploring genetic interaction manifolds constructed from rich single-cell phenotypes. Science. 2019;365:786–93.
32. Doench JG. Am I ready for CRISPR? A user's guide to genetic screens. Nat Rev Genet. 2018;19:67–80.
33. Gilbert LA, Larson MH, Morsut L, Liu Z, Brar GA, Torres SE, et al. CRISPR-mediated modular RNA-guided regulation of transcription in eukaryotes. Cell. 2013;154:442–51.
34. Gilbert LA, Horlbeck MA, Adamson B, Villalta JE, Chen Y, Whitehead EH, et al. Genome-scale CRISPR-Mediated control of gene repression and activation. Cell. 2014;159:647–61.
35. Horlbeck MA, Gilbert LA, Villalta JE, Adamson B, Pak RA, Chen Y, et al. Compact and highly active next-generation libraries for CRISPR-mediated gene repression and activation. eLife. 2016;5:e19760.
36. Qi LS, Larson MH, Gilbert LA, Doudna JA, Weissman JS, Arkin AP, et al. Repurposing CRISPR as an RNA-guided platform for sequence-specific control of gene expression. Cell. 2013;152:1173–83.
37. Replogle JM, Norman TM, Xu A, Hussmann JA, Chen J, Cogan JZ, et al. Combinatorial single-cell CRISPR screens by direct guide RNA capture and targeted sequencing. Nat Biotechnol. 2020;38:954–61.
38. Guna A, Hazu M, Tomaleri GP, Voorhees RM. A TAle of two pathways: tail-anchored protein insertion at the endoplasmic reticulum. Cold Spring Harb Perspect Biol. 2022;15:a041252.
39. Kutay U, Hartmann E, Rapoport TA. A class of membrane proteins with a C-terminal anchor. Trends Cell Biol. 1993;3:72–5.
40. Stefanovic S, Hegde RS. Identification of a targeting factor for posttranslational membrane protein insertion into the ER. Cell. 2007;128:1147–59.
41. Schuldiner M, Metz J, Schmid V, Denic V, Rakwalska M, Schmitt HD, et al. The GET complex mediates insertion of tail-anchored proteins into the ER membrane. Cell. 2008;134:634–45.
42. Guna A, Volkmar N, Christianson JC, Hegde RS. The ER membrane protein complex is a transmembrane domain insertase. Science. 2018;359:470–3.
43. Vilardi F, Stephan M, Clancy A, Janshoff A, Schwappach B. WRB and CAML are necessary and sufficient to Mediate tail-anchored protein targeting to the ER membrane. PLoS ONE. 2014;9:e85033.
44. Vilardi F, Lorenz H, Dobberstein B. WRB is the receptor for TRC40/Asna1-mediated insertion of tail-anchored proteins into the ER membrane. J Cell Sci. 2011;124:1301–7.
45. Wang F, Brown EC, Mak G, Zhuang J, Denic V. A chaperone cascade sorts proteins for posttranslational membrane insertion into the endoplasmic reticulum. Mol Cell. 2010;40:159–71.
46. Rao M, Okreglak V, Chio US, Cho H, Walter P, Shan S. Multiple selection filters ensure accurate tail-anchored membrane protein targeting. eLife. 2016;5:e21301.
47. Shao S, Rodrigo-Brenni MC, Kivlen MH, Hegde RS. Mechanistic basis for a molecular triage reaction. Science. 2017;355:298–302.
48. Görlich D, Prehn S, Hartmann E, Kalies K-U, Rapoport TA. A mammalian homolog of SEC61p and SECYp is associated with ribosomes and nascent polypeptides during translocation. Cell. 1992;71:489–503.
49. Görlich D, Rapoport TA. Protein translocation into proteoliposomes reconstituted from purified components of the endoplasmic reticulum membrane. Cell. 1993;75:615–30.
50. Esnault Y, Blondel MO, Deshaies RJ, Scheckman R, Kepes F. The yeast SSS1 gene is essential for secretory protein translocation and encodes a conserved protein of the endoplasmic reticulum. EMBO. 1993;12:4083–93.
51. Inglis AJ, Page KR, Guna A, Voorhees RM. Differential modes of Orphan Subunit Recognition for the WRB/CAML complex. Cell Rep. 2020;30:3691–3698e5.
52. Guna A, Stevens TA, Inglis AJ, Replogle JM, Esantsi TK, Muthukumar G, et al. MTCH2 is a mitochondrial outer membrane protein insertase. Science. 2022;378:317–22.
53. Volkmar N, Thezenas M-L, Louie SM, Juszkiewicz S, Nomura DK, Hegde RS et al. The ER membrane protein complex promotes biogenesis of sterol-related enzymes maintaining cholesterol homeostasis. J Cell Sci. 2019;132.
54. Pleiner T, Hazu M, Tomaleri GP, Januszyk K, Oania RS, Sweredoski MJ, et al. WNK1 is an assembly factor for the human ER membrane protein complex. Mol Cell. 2021;81:2693–704. e12.
55. Coukos R, Yao D, Sanchez MI, Strand ET, Olive ME, Udeshi ND, et al. An engineered transcriptional reporter of protein localization identifies regulators of mitochondrial and ER membrane protein trafficking in high-throughput. … eLife. 2021;10:e69142.
56. Adamson B, Norman TM, Jost M, Cho MY, Nuñez JK, Chen Y, et al. A multiplexed single-cell CRISPR screening platform enables systematic dissection of the unfolded protein response. Cell. 2016;167:1867–1882e21.
57. van de Weijer ML, Krshnan L, Liberatori S, Guerrero EN, Robson-Tull J, Hahn L, et al. Quality control of ER membrane proteins by the RNF185/membralin ubiquitin ligase complex. Mol Cell. 2020;79:768–81. e7.
58. Xu Y, Liu Y, Lee J, Ye Y. A ubiquitin-like domain recruits an oligomeric chaperone to a retrotranslocation complex in endoplasmic reticulum-associated degradation. J Biol Chem. 2013;288:18068–76.
59. Lee JN, Zhang X, Feramisco JD, Gong Y, Ye J. Unsaturated fatty acids inhibit proteasomal degradation of Insig-1 at a postubiquitination step. J Biol Chem. 2008;283:33772–83.
60. Feng X, Tang M, Dede M, Su D, Pei G, Jiang D, et al. Genome-wide CRISPR screens using isogenic cells reveal vulnerabilities conferred by loss of Tumor suppressors. Sci Adv. 2022;8:eabm6638.
61. Westermann L, Li Y, Göcmen B, Niedermoser M, Rhein K, Jahn J, et al. Wildtype heterogeneity contributes to clonal variability in genome edited cells. Sci Rep. 2022;12:1–13.
62. Rossi A, Kontarakis Z, Gerri C, Nolte H, Hölper S, Krüger M, et al. Genetic compensation induced by deleterious mutations but not gene knockdowns. Nature. 2015;524:230–3.
63. Alerasool N, Segal D, Lee H, Taipale M. An efficient KRAB domain for CRISPRi applications in human cells. Nat Methods. 2020;17:1093–6.
64. Replogle JM, Bonnar JL, Pogson AN, Liem CR, Maier NK, Ding Y, et al. Maximizing CRISPRi efficacy and accessibility with dual-sgRNA libraries and optimal effectors. eLife. 2022;11:e81856.
65. Leto DE, Morgens DW, Zhang L, Walczak CP, Elias JE, Bassik MC, et al. Genome-wide CRISPR Analysis identifies substrate-specific Conjugation modules in ER-Associated Degradation. Mol Cell. 2019;73:377–389e11.
66. Tsai PL, Cameron CJF, Forni MF, Wasko RR, Naughton BS, Horsley V, et al. Dynamic quality control machinery that operates across compartmental borders mediates the degradation of mammalian nuclear membrane proteins. Cell Rep. 2022;41:111675.
67. Morita K, Hama Y, Izume T, Tamura N, Ueno T, Yamashita Y, et al. Genome-wide CRISPR screen identifies TMEM41B as a gene required for autophagosome formation. J Cell Biol. 2018;217:3817–28.
68. Jost M, Chen Y, Gilbert LA, Horlbeck MA, Krenning L, Menchon G, et al. Combined CRISPRi/a-based chemical genetic screens reveal that rigosertib is a microtubule-destabilizing agent. Mol Cell. 2017;68:210–23. e6.
69. Chitwood PJ, Juszkiewicz S, Guna A, Shao S, Hegde RS. EMC is required to initiate accurate membrane protein topogenesis. Cell. 2018;175:1507–19. e16.

70. Cabantous S, Terwilliger TC, Waldo GS. Protein tagging and detection with engineered self-assembling fragments of green fluorescent protein. Nat Biotechnol. 2005;23:102–7.
71. Kamiyama D, Sekine S, Barsi-Rhyne B, Hu J, Chen B, Gilbert LA, et al. Versatile protein tagging in cells with split fluorescent protein. Nat Commun. 2016;7:11046.
72. Landisman CE, Connors BW. Long-term modulation of electrical synapses in the mammalian thalamus. Science. 2005;310:1809–13.
73. Stewart SA, Dykxhoorn DM, Palliser D, Mizuno H, Yu EY, An DS, et al. Lentivirus-delivered stable gene silencing by RNAi in primary cells. RNA. 2003;9:493–501.

Publisher's Note